



Composition dependent selectivity of bimetallic Au-Pd NPs immobilised on titanate nanotubes in catalytic oxidation of glucose

Motaz Khawaji^a, Yiming Zhang^a, Melody Loh^a, Inês Graça^a, Ecaterina Ware^b, David Chadwick^{a,*}

^a Department of Chemical Engineering, Imperial College London, London, SW7 2AZ, United Kingdom

^b Department of Materials, Royal School of Mines, Imperial College London, London, SW7 2AZ, United Kingdom



ARTICLE INFO

Keywords:

Glucose
Selective oxidation
Au-Pd
Titanate nanotubes
Sol-Immobilisation

ABSTRACT

The catalytic performance of Au-Pd nanoparticles (NP) prepared by colloidal synthesis and immobilised on titanate nanotubes (Ti-NT) in the selective oxidation of glucose to gluconic and glucaric acids has been studied under initially basic and relatively mild conditions. Catalysts with varying compositions displayed quite different product selectivity especially in relation to deeper oxidation. The yield of glucaric acid was found to be proportional to the atomic content of Au in the Au-Pd NPs: Au/Ti-NT exhibited the highest selectivity to glucaric acid, while Au₁₅Pd₈₅/Ti-NT displayed the highest selectivity to gluconic acid, $S_{GLO} > 98\%$. Catalyst recycling revealed deactivation, which appears to be due to a combination of metal leaching, particle size changes and product adsorption, and is associated with the gradual fall in pH of the reaction mixture. Results suggest that the leached Au species play a significant role in the oxidation of gluconic to glucaric acid.

1. Introduction

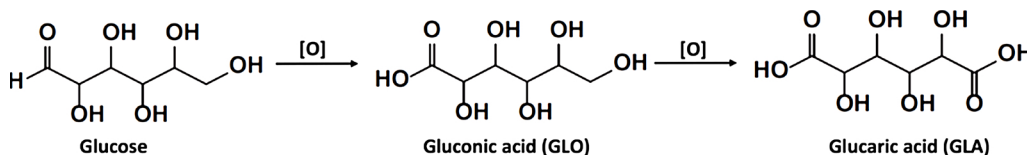
The transformation and valorisation of sustainable bio-renewable resources into chemical products has been the subject of intense research in recent years. Sugars derived from abundant biomass resources have the potential to serve as a versatile platform for the production of numerous high-value chemicals [1]. The selective oxidation of glucose (**Scheme 1**) to gluconic acid (GLO), and its subsequent oxidation to glucaric acid (GLA) are potentially key steps in the biomass-to-chemicals value chain. Gluconic acid and its salts are valuable compounds with numerous applications in the food and beverages, pharmaceuticals, textile and papermaking industries [2–4]. At present, gluconic acid and its salts (i.e. gluconates) are produced primarily through the enzymatic oxidation of glucose with *Aspergillus niger* fungus [2]. However, this production route has several drawbacks namely the low activity, high cost of enzymes separation and waste-water disposal [5]. Glucaric acid (GLA) and its glucarate salts are also valuable chemicals. GLA has been classified by the U.S. Department of Energy as one of the “top value-added chemicals” that can be derived from biomass [6]. It can be used for instance in the formulation of detergents [6], and as a potential intermediate in the production of bio-derived adipic acid [7,8]. The current commercial production of GLA relies predominantly on the use of nitric acid for the oxidation of glucose [9,10]. The nitric acid process is moderately selective and environmentally unfriendly.

However, it remains the most economic route for the production of GLA from glucose [11]. Evidently, the current routes for commercial production of GLO and GLA suffer from several shortcomings, and hence the development of more sustainable and efficient processes is important for large-scale application. The direct catalytic selective oxidation of glucose under mild conditions using air or molecular oxygen and supported metal catalysts is a potentially attractive alternative for the production of GLO and GLA which could have a lower environmental impact.

The oxidation of glucose with air, oxygen or hydrogen peroxide and heterogeneous catalysts mainly to gluconic acid or its salts has been studied for many years most notably over Pt or Pd supported on carbon, and also with the addition of various promoters such as Bi with aim of mitigating deactivation or suppressing the formation of the undesired 2-ketogluconic acid [5,12–14]. More recently, gold and gold alloys have been shown to be good catalysts for the oxidation of glucose to gluconic acid [15–17]. The activity and selectivity of Au NPs in the aerobic oxidation of carbohydrates (e.g. glucose) has been attributed to the ability of gold to resist oxygen poisoning and to convert the aldose groups to their corresponding aldonic acids (e.g. gluconic acid) [18,19]. The optimum pH for the selective oxidation of glucose to gluconic acid with transition metal catalysts is typically 9–11. At this pH lactone formation is largely avoided, and metal leaching and catalyst deactivation are minimised. High pH is typically achieved by the addition of a

* Corresponding author.

E-mail address: d.chadwick@imperial.ac.uk (D. Chadwick).



Scheme 1. Selective oxidation of glucose to gluconic acid (GLO) and glucaric acid (GLA).

sacrificial base such as NaOH [15,20]. Mild conditions are favoured for the selective oxidation of glucose to gluconic acid with the optimum reaction temperature being around 50 °C [3]. Selectivity to gluconic acid exceeding 98% can be achieved at these conditions. Early studies used carbon as support, but recently the use of TiO₂ has gained in popularity due to its widespread use as a support in selective oxidation reactions [21]. The addition of base can lead to undesired waste streams and as a consequence there have been a number of recent reports on the selective oxidation of glucose under base-free conditions with heterogeneous catalysts [18,21]. The aim of these studies is to produce pure gluconic acid rather than the salt and to eliminate the use of base, motivated as noted above primarily by environmental concerns.

Most of the literature has focused on the oxidation of glucose to GLO in which very small or near zero yield of GLA was reported [16,22] [23]. Recently, interest in the production of GLA from glucose has assumed greater prominence as it has been recognised as an important platform molecule in its own right and a key intermediate in the route from sugars to adipic acid. For example, Rennovia Inc. claimed GLA production using a range of Pt supported catalysts [24,25]. Glucaric acid yields of up ca. 70% were reported at T = 80–100 °C and oxygen pressure of 6 bar in acetic solution. However, significant lactone formation was noted at these acidic conditions. Catalysts containing gold did not perform well and indeed catalysts based on Au are not expected to be the most promising in acidic conditions. In general, oxidation of glucose to glucaric acid is favoured by higher reaction temperature and oxygen pressure than for oxidation to gluconic acid. Nevertheless, the reaction is still relatively slow and therefore the need for more efficient and/or selective catalysts persists. Recently, Jin et al. [26] reported a highly active Pt₁Cu₃/TiO₂ catalyst for oxidation to glucaric acid. A surface TOF of 3543 h⁻¹ was achieved at 45 °C for oxidation of Na gluconate with a selectivity to glucarate of 45% due to a significant fraction of tartronic and oxalic acids as well as some monocarboxylic acids as a result of the cleavage of C–C bonds. However, it is important to note that the high TOF value was obtained in the presence of very strong base (1 M NaOH or pH > 13) which enhances the activity very significantly. Lee et al. reported a GLA yield as high as 74% over Pt/C depending on the conditions [27].

In principle, separation of gluconate and glucarate salts is easier than the separation of the free acids. Base conditions also lead to the minimisation of lactone formation [11]. Indeed, studies have shown that lactonization of gluconic and glucaric acids to lactones and dilactones can occur readily at low pH values and temperatures as low as 50 °C [28,29]. Armstrong et al. [30] have recently developed a new process based on ion exchange and azeotropic evaporation for the derivation of high purity glucaric acid (> 99.96%) directly from the glucarate salts. This newly-reported process is significant because it facilitates the direct conversion of more readily obtainable glucarate salts to high purity crystalline glucaric acid and avoids formation of lactone and dilactone glucarate derivatives, which can be formed during separation and water removal. In principle, the recovered base could be recycled avoiding excessive waste streams. Therefore, the use of base in the catalytic oxidation of glucose can be justified on the basis of catalytic performance and ease of product separation. The use of a high pH makes Au-based catalysts attractive for glucose selective oxidation.

It is well-known that the catalytic activity of gold catalysts is strongly dependent on the gold particle size, catalyst preparation

method, and the nature of the support. The effect of the catalyst preparation method and Au NP size on activity in glucose oxidation have been previously reported [31,32]. Hutchings and co-workers found that the catalyst preparation method was crucial for the catalytic activity of supported Au catalysts for glucose oxidation, and that sol-immobilisation produces the best Au catalyst [21]. Haurta and co-workers investigated the oxidation of glucose using Au NPs supported on various materials (carbon, Al₂O₃, ZrO₂, TiO₂, CeO₂), and concluded that the Au particle and catalyst preparation method influence the catalytic activity more significantly than the nature of the support and the metal-support interaction [33]. We have recently reported on the high catalytic activity of bimetallic Au-Pd NPs prepared by colloidal synthesis and immobilised on titanate nanotubes (Ti-NT) for the selective oxidation of benzyl alcohol [34]. We have demonstrated how the morphology and structure of titanate nanotubes influence the catalytic activity and lead to a more active catalyst in comparison with the equivalent catalyst supported on a conventional titania nanopowder. Ti-NT possess a large surface area and a high surface hydroxyl group density of ca. 5.8 OH/nm² [35]. These physiochemical and morphological properties make Ti-NT very attractive as a catalyst support. The high population of surface –OH groups in Ti-NT can be utilised as anchoring sites for Au-Pd colloidal NPs [34]. It has also been demonstrated that by using the sol-immobilisation method, the Au-Pd NPs are located on the external surfaces of Ti-NT as opposed to the internal pore volume or interstitial sites of Ti-NT [36], allowing easy accessibility of the reactants to the active metal sites, and product escape, which is potentially important for reactions involving molecules such as glucose and fructose and their derivatives. Therefore, Au-based catalysts using Ti-NT as support would appear to be potentially attractive materials for glucose oxidation.

In this paper we report the catalytic performance of Au_xPd_y/Ti-NT in the selective oxidation of glucose under relatively mild and basic conditions with molecular oxygen. The catalysts have been prepared by immobilisation of colloidal Au, Pd and Au-Pd NPs with different atomic composition (Au_xPd_y, where x = Au at.% and y = Pd at.%) on Ti-NT since as noted above this method yields highly active catalysts. Of particular interest is the catalytic activity and selectivity to glucaric acid and the dependence on the bimetallic composition. The high dispersion and high degree of alloying in the Au-Pd NPs on the Ti-NT support make these ideal materials to examine the dependence on bimetallic alloy composition. It is shown that under initially basic conditions, the addition of even a relatively small proportion of Au atoms to Pd NPs leads to significant enhancement in the catalytic activity and the selectivity to glucaric acid. For the first time it is shown that the yield of GLA acid is close to linearly dependent on the atomic composition of Au in the Au-Pd catalysts. The deactivation and recycling of the Au/Ti-NT and Au₁₅Pd₈₅/Ti-NT catalysts have been investigated, and the possible catalytic role of the leached material has also been studied briefly.

2. Materials and methods

2.1. Materials

All metal precursors and chemical reagents were purchased from Sigma Aldrich and used as received unless otherwise noted: NaOH (99.99% trace metals basis), H₂SO₄ (≥ 97.5% purity), TiO₂ (Aerioxide P25), Pt/SiO₂ (5 wt.% Pt supported on silica), Pt/C (5 wt.% Pt supported on activated carbon), poly(vinyl alcohol) (PVA) (MW

9,000–10,000, 80% hydrolysed), HAuCl₄·3H₂O (99.999% purity), PdCl₂ (5 wt. % in 10 wt. % HCl), NaBH₄ (≥98.0%), D-glucose (> 99.5% purity), gluconic acid (49–53 wt. % in H₂O); glycolic acid (99% purity); oxalic acid (≥99.0% purity); fructose (≥ 99% purity). Glucaric acid with 99.96% purity was provided by Cardiff Catalysis Institute [28]. Oxygen (100% pure) for catalytic tests was supplied by BOC.

2.2. Catalyst synthesis

2.2.1. Synthesis of titanate nanotubes (Ti-NT)

Titanate Nanotubes (Ti-NTs) were synthesised by the alkaline hydrothermal treatment reported by Kasuga et al. [37]. In a typical synthesis, 11.0 g of TiO₂ (anatase nanopowder) was added to 185 mL (10 M NaOH) in a 200 mL PTFE-liner and stirred for two hours. The PTFE-lined steel autoclave was then placed in an oven at 140 °C for 24 h. The obtained slurry was then washed with DI water, filtered and dried overnight at 120 °C. The dried powder was washed with 0.1 M H₂SO₄ and filtered. This process was repeated until pH 7 was reached. Finally, the Ti-NT powder was washed thoroughly with DI water to remove any residual Na or H₂SO₄, and dried overnight at 120 °C.

2.2.2. Catalysts preparation

Catalysts supported on Ti-NT were prepared in a manner similar to the sol-immobilisation procedure previously reported [34,38]. First, the Ti-NTs were acidified to a pH below the point of zero charge (PZC) of Ti-NT. Typically, 1.0 g of the support was added to 75 mL of water and a solution of H₂SO₄ (1.0 M) was added drop-wise to the slurry until the pH dropped to 1.5. The Au, Pd and bimetallic Au-Pd colloidal NPs were prepared by dissolving calculated amounts of HAuCl₄·3H₂O and PdCl₂ corresponding to a nominal metal loading of 2.0 wt.% in 100 mL of DI water at 5 °C while stirring vigorously. The amounts of metal precursors added were as follows: Au/Ti-NT (HAuCl₄·3H₂O = 0.102 mmol), Pd/Ti-NT (PdCl₂ = 0.189 mmol), Au₅₆Pd₄₄/Ti-NT (HAuCl₄·3H₂O = 0.077, PdCl₂ = 0.047 mmol), Au₃₃Pd₆₇/Ti-NT (HAuCl₄·3H₂O = 0.051 mmol, PdCl₂ = 0.094 mmol), and Au₁₅Pd₈₅/Ti-NT (HAuCl₄·3H₂O = 0.026 mmol, PdCl₂ = 0.142 mmol). Catalyst sample Au/TiO₂ was prepared using TiO₂ P25 as a support, and the same sol-immobilisation procedure used as for Au/Ti-NT. The nominal loading was calculated on the basis of the amount of metal precursors added to the solution assuming 100% conversion of the metal precursors to the supported metals.

Subsequently, a specified amount of 1.0 wt.% PVA solution was added to the metal precursors solution and stirred for a few minutes. The weight ratio of PVA/(M) was kept at 1.20 for all catalysts, (M = Au, Pd or Au + Pd). The metal precursors were reduced by the addition of 0.1 M NaBH₄ (molar ratio of NaBH₄ : M = 5 : 1). The metal colloid was left stirring at 1500 rpm for one hour before the acidified Ti-NT was added. The slurry was stirred for one hour before it was filtered and washed with DI water until the final pH of the mother liquor reached ~7.0. The obtained catalysts were subsequently dried overnight at 100 °C, and then refluxed in hot water (90 °C) for 60 min, filtered and dried overnight at 100 °C. The dried catalysts were used as is without any further treatment. The bimetallic catalysts were denominated using their nominal atomic composition (Au₅₆Pd₄₄/Ti-NT, Au₃₃Pd₆₇/Ti-NT and Au₁₅Pd₈₅/Ti-NT).

Catalyst Au-Pd/TiO₂ was prepared by dry impregnation of 1.0 g of TiO₂ P25 with the requisite amounts HAuCl₄·3H₂O (0.051 mmol) and PdCl₂ (0.094 mmol). The metal precursors were dissolved in 0.3 mL DI water (the volume of DI water to give a surface loading [39] of ~200,000 m²/L). The precursor solution was added drop-wise to the support to form a fine paste. The paste was dried overnight at 100 °C. The catalyst was finally reduced for 2 h at 200 °C in a tube furnace under a continuous flow of diluted hydrogen (5 vol.% H₂/N₂). The furnace ramp rate was set to 5 °C/min, and gas flow rate was fixed at ~50 mL/min.

2.3. Reaction procedure

Glucose oxidation was conducted using a 25 mL glass-lined mini-clave (Buchiglas, Switzerland) batch reactor. Typically, glucose solution (3.0 mL, 0.25 M, pH_{initial} = 9.5) and the requisite amount of catalyst were added to the reactor. The glucose: catalytic metal molar ratio was kept at 100:1, and Na:glucose = 1:7900 mol/mol. The glass reactor was purged three times with pure O₂ before being pressurised to the desired pressure (5 barg at room temperature). Subsequently, the temperature of the reactor was set to 80 °C, and reactor was stirred at 1000 rpm. At the end of each run, the reactor was cooled down to room temperature and vented slowly. Subsequently, 7.0 mL DI water was added to the reactor to dilute the product mixture. The liquid phase was separated from catalyst by centrifugation at 5000 rpm for 20 min. A sample (7.0 mL) was taken from the supernatant and was mixed with 50 µL formic acid (internal standard) prior to product analysis. Product analysis was carried out using HPLC (CTO-20AC, Shimadzu, Japan) fitted with a SUPELCOGEL™ C-610H HPLC column (30 cm x 7.8 mm ID, filter: 25 mm ID with 0.45 µm pores) and equipped with UV and refractive index detectors. A solution with 0.1% v/v phosphoric acid was used as the mobile phase. The instrument was calibrated with high purity standards purchased from Sigma Aldrich prior to product analysis. Products were identified using HPLC. The spent catalyst was collected at the end of each run and washed several times with a mixture of water and ethanol, and centrifuged before it was dried overnight at 90 °C. The dried catalyst was then used for the next reaction cycle. The conversion of glucose (X_G), product yield (Y_i), selectivity (S_i), and carbon balance were calculated using the following equations:

$$X_G (\%) = \frac{n_{\text{initial glucose}} - n_{\text{final glucose}}}{n_{\text{initial glucose}}} \times 100$$

$$Y_i (\text{mol}\%) = \frac{n_{\text{product } i}}{n_{\text{initial glucose}}} \times 100$$

$$S_i (\text{mol}\%) = \frac{n_{\text{product } i}}{\sum_{i=1}^j n_{\text{product } i}} \times 100$$

$$\text{Carbon balance} (\%) = \frac{\text{initial moles of carbon}}{\text{final moles of carbon}} \times 100$$

Where *n* is the number of moles of glucose or carbon containing product *i*.

2.4. Catalyst characterisation

X-ray diffraction (XRD) measurements were recorded using a PANalytical X'Pert Pro Multi-Purpose Diffractometer using CuK α radiation. The analysis was performed over a scan angle of 2θ = 5–70°, and a step size 0.0167°. The bulk metal loading was determined by inductively coupled plasma atomic emission spectroscopy (ICP-AES, PE Optima 2000 DV). Typically, the catalyst (12–15 mg) was dissolved in aqua regia (15 mL), sonicated for 2 h and diluted with de-ionised water prior to analysis. Bright-field TEM images were obtained using a JEOL JEM-2100F microscope operating at 200 kV. Samples were dispersed in ethanol and sonicated for 30 min before they were placed on copper grids with a lacy carbon film (300 mesh size). The average particle size and particle size distribution of the metal NPs were determined from the TEM images by analysing 100 randomly selected metal NPs. X-ray photoelectron spectroscopy (XPS) measurements were recorded using a Thermo K-Alpha Spectrometer equipped with Al K α source gun. Samples were mounted on adhesive carbon tape, and the spectra were collected using an X-ray spot size of 400 µm with a pass energy of 20 eV and 0.1 eV increments. The binding energies (BE) were referenced to the C 1s peak of adventitious carbon at 284.8 eV. The XPS data were analysed using Avantage software from Thermo Scientific. The error in the XPS measurement is typically ± 0.2 eV.

3. Results and discussion

3.1. Catalyst preparation and characterisation

The formation of the titanate nanotubes supports synthesized by alkaline hydrothermal treatment was confirmed by XRD, nitrogen adsorption-desorption measurements, and TEM. The XRD patterns of the as-synthesised Ti-NT is shown in Fig. S1a in the Electronic Supplementary Information (ESI). Titanate nanotubes are characteristically identified by the emergence of a broad angle peak between 7.2 and 10.3° 2θ in the XRD pattern, which have been ascribed to the interlayer spacing of the layered titanate phase. The peaks at 24.5°, 28.6° and 48.6° are also characteristic of tri-titanate 1D nanomaterials [40,41]. The intensity of the small peak at 28.6° is observed to vary slightly from batch to batch of Ti-NT [36]. The Ti-NT used in the preparation of the catalysts had a BET surface area ca. 236 m²/g, which is a typical value for hydrothermally-synthesized protonated Ti-NT. The formation of Ti-NT was also confirmed by TEM whereby the nanotubular morphology of Ti-NT is clearly visible in the TEM images (Fig. S1b).

Au, Pd and Au-Pd colloidal NPs with various Pd/Au ratios were prepared and immobilised on the surfaces of Ti-NT. Table 1 gives the metal composition and textural properties of the different catalysts prepared in the present study. All the catalysts were prepared by sol-immobilisation with the exception of the benchmark catalyst (i.e. Au-Pd/TiO₂) which was prepared by conventional dry impregnation. The actual metal loading of the catalysts was determined by ICP-AES and was found to be close to the nominal loading (Table 1) for all catalysts, which indicates that most of the metal NPs were adsorbed by the Ti-NT support. The surface areas of the catalysts were close to that of the Ti-NT support indicating that no major changes in the textual properties of Ti-NT were induced during catalyst preparation.

The XRD diffraction patterns of the catalysts and Ti-NT support are shown in Fig. 1. The monometallic gold catalyst (i.e. Au/Ti-NT) displayed a relatively weak and broad peak at 38.41°, which can be assigned to the pure Au(111) reflection. The bimetallic catalysts (Au_xPd_y/Ti-NT) displayed Au(111) peaks at higher 2θ, which is a result of the change in the lattice constant and confirms the formation of a Pd-Au alloy phase in these catalysts [42]. It is well-known that Au and Pd are completely miscible in each other with a continuous range of solubility [43,44]. The magnitude of the 2θ shift was proportional to the amount of Pd present in the catalyst with the largest shift observed for Au₁₅Pd₈₅/Ti-NT, see the inset of Fig. 1. No other clear diffraction peaks corresponding to Au or Pd diffraction planes were observed in any of the catalysts owing to the low metal concentration and relatively small particle size of the metal NPs. The Au(111) peak for Au-Pd/TiO₂ could not be identified clearly because it overlaps with the reflections of the anatase and rutile phases present in TiO₂ P25 (Fig. S2 in ESI).

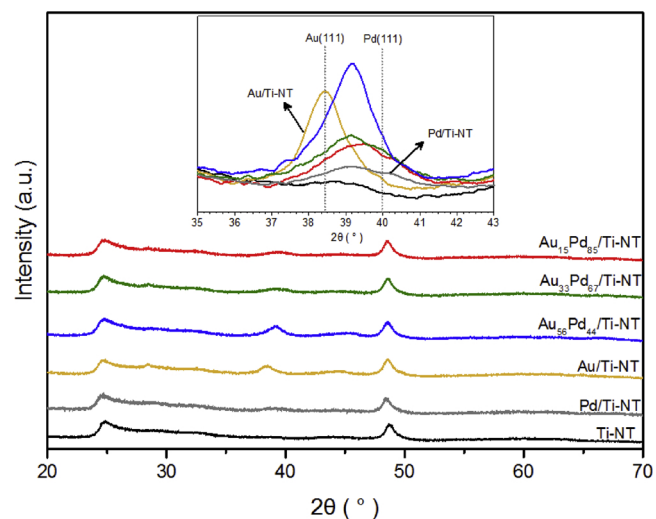


Fig. 1. X-ray diffraction patterns for the different Au-Pd/Ti-NT catalysts prepared in the study. Inset shows the shift of the Au(111) diffraction peak due to alloy formation.

HRTEM images (Fig. 2) revealed information about the structure and morphology of the catalysts, as well as the particle size distribution (PSD) of the metal NPs on the surface of Ti-NT. The dried samples of Ti-NT have tendency to aggregate, especially after catalyst synthesis involving PVA. The monometallic Au and Pd catalysts (Fig. 2a and b) exhibited a mean particle size that is smaller than all the bimetallic Au_xPd_y/Ti-NT catalysts. In particular, Au/Ti-NT displayed the smallest mean particle size (ca. 3.2 nm) with most Au NPs falling between 2.5–4 nm in size, although occasional particles with larger sizes were observed. Nonetheless, all the bimetallic and monometallic catalysts displayed narrow PSD and relatively small mean particle size, which highlights an advantage of using colloidal synthesis over the more traditional synthesis methods. We have previously shown that by using the sol-immobilisation procedure [34], Au-Pd NPs are attached almost exclusively on the external surfaces of Ti-NT as opposed to the inner pores or the inertial sites, and this is also clearly demonstrated in the HRTEM image shown in Fig. S3. The catalyst prepared by sol-immobilisation of Au NPs on TiO₂ P25 (i.e. Au/TiO₂) exhibited a mean particle size of 4.5 nm, which is larger than Au/Ti-NT. The conventional Au-Pd/TiO₂ catalyst prepared by dry impregnation displayed poor dispersion with frequent large metal NPs (see Fig. S4 in the ESI). The properties of the support material ultimately determine the final size of the metal NPs and their dispersion on the support [45]. The larger particle sizes seen for TiO₂ P25, even for catalysts prepared by sol-immobilisation, in part reflects the lower surface area of the TiO₂ P25 support.

Table 1
Metal composition, textural and physicochemical properties of the various prepared catalysts.

Catalyst	Au (wt.%)		Pd (wt.%)		weight ratio Pd/Au	S _{BET} ^b (m ² /g)	Metal dispersion ^c (%)
	nominal	actual ^a	nominal	actual ^a			
Au/Ti-NT	2.0	1.61	–	–	–	226	36
Pd/Ti-NT	–	–	2.0	1.45	–	230	28
Au ₅₆ Pd ₄₄ /Ti-NT	1.5	1.27	0.5	0.54	0.43	216	25
Au ₃₃ Pd ₆₇ /Ti-NT	1.0	0.70	1.0	0.78	1.11	217	31
Au ₁₅ Pd ₈₅ /Ti-NT	0.5	0.46	1.5	1.37	2.98	217	27
Au/TiO ₂ ^d	2.0	1.45	–	–	–	54	31
Au-Pd/TiO ₂ ^e	1.0	0.82	1.0	0.91	1.10	51	–

^a Bulk composition; weight percentage per gram of sample, obtained by ICP-AES analysis.

^b Determined by nitrogen adsorption-desorption measurements.

^c Determined from the particle size distribution as determined from TEM.

^d Catalyst prepared by dry sol-immobilisation.

^e Catalyst prepared by dry impregnation.

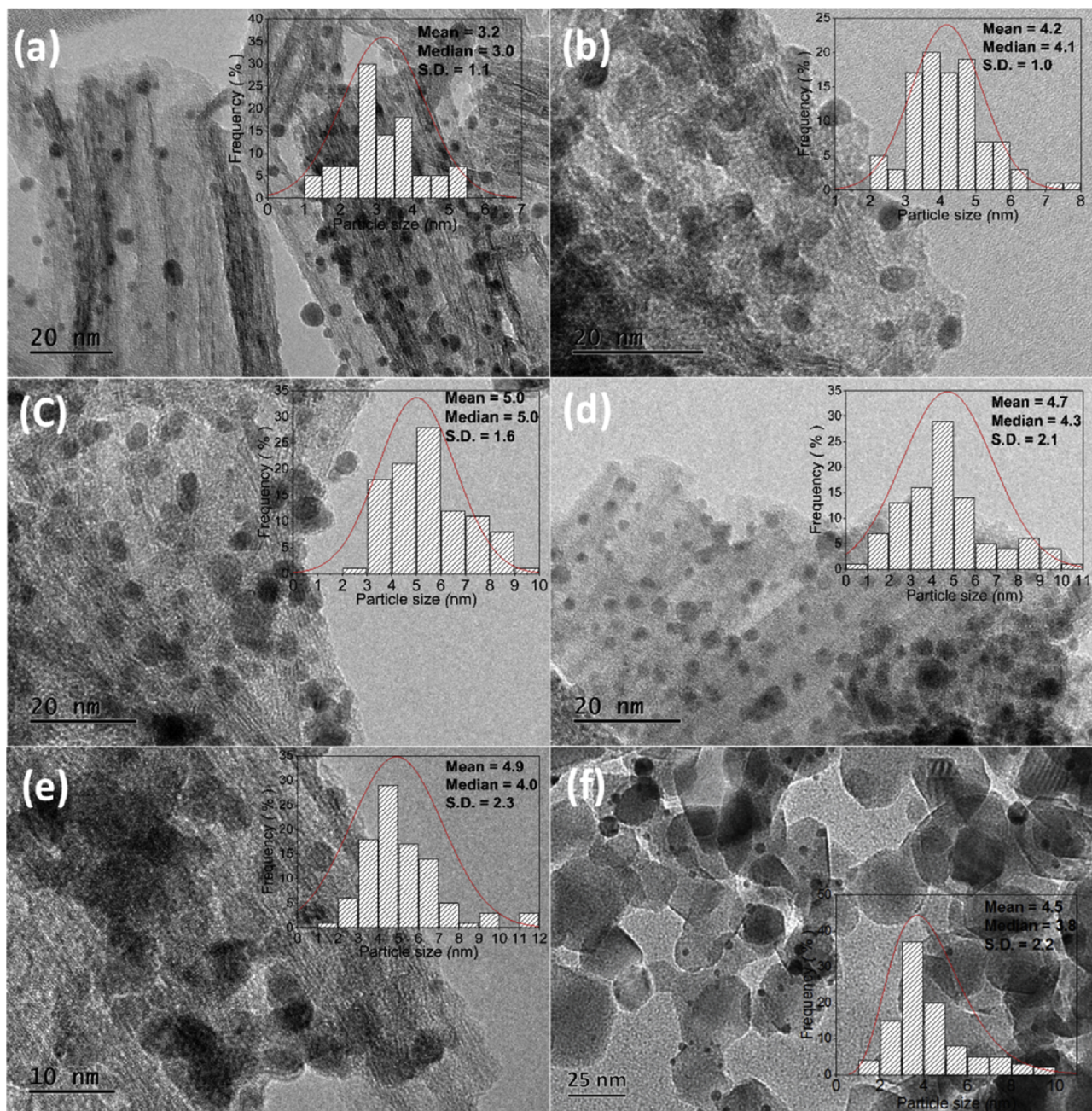


Fig. 2. HRTEM images of catalyst sample (a) Au/Ti-NT, (b) Pd/Ti-NT, (c) Au₅₆Pd₄₄/Ti-NT, (d) Au₃₃Pd₆₇/Ti-NT, (e) Au₁₅Pd₈₅/Ti-NT, and (f) Au/TiO₂. The inset in each figure represents the corresponding particle size distribution.

The metal dispersion (%) shown in Table 1 was calculated using the approximation method reported by Mori et al. [46] and the particle size distribution determined from TEM. All metal NPs were assumed to be face-centred cubic (FCC) cub-octahedral in shape [46]. Au/Ti-NT displayed the highest metal dispersion, followed by Pd/Ti-NT. The bimetallic catalysts displayed nearly the same metal dispersion; that it was not dependent on the Au-Pd ratio.

The surface atomic compositions and oxidation states of Au and Pd on the surface of the catalysts were investigated by XPS. The XPS spectra for Au 4f and Pd 3d are shown in Figs. 3 and 4 respectively. The binding energy (B.E.) of the Au 4f_{7/2} component for the monometallic gold catalyst (Au/Ti-NT) was observed at 83.4 eV, while the bimetallic catalysts (Au_xPd_y/Ti-NT) exhibited Au 4f_{7/2} peaks at lower binding energies. The negative peak shift in the B.E. can be ascribed to the electronic modification of Au species by Pd and is indicative of the close

interaction between the Au and Pd atoms and the formation of an Au-Pd alloy phase. This finding is in agreement with the XRD results above. Recent consensus in literature regarding the B.E. shift point to a net charge transfer from Pd to Au [42,44,47]. The Au 4f spectra show that gold exists predominantly as Au⁰ in the catalyst samples, although the slight broadening to higher B.E. may indicate the presence of either oxidised gold species (Au⁸⁺) or very small gold NPs not seen in the TEM images [48].

The Pd 3d spectra for Pd/Ti-NT and Au_xPd_y/Ti-NT catalysts point to the presence of metallic palladium (Pd⁰) as well as oxidised palladium species in the dried catalysts. The Pd 3d spectra were deconvoluted using one component corresponding to Pd⁰ and two components corresponding to Pd²⁺ and Pd⁴⁺ (Fig. 4). The B.E. for the Pd 3d_{5/2} component of Pd⁰ in these catalysts falls between 334.9 and 334.7 eV (Table 2). The oxidised Pd species appear at higher B.E. between ca.

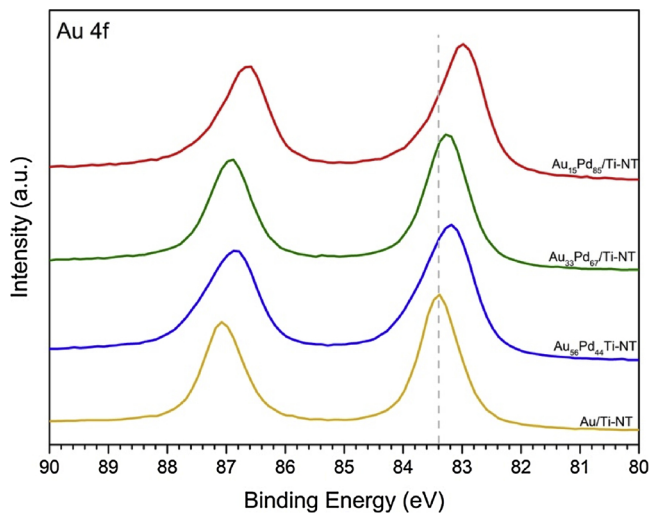


Fig. 3. XPS spectra of Au 4f for Au/Ti-NT and $\text{Au}_x\text{Pd}_y/\text{Ti-NT}$ catalysts.

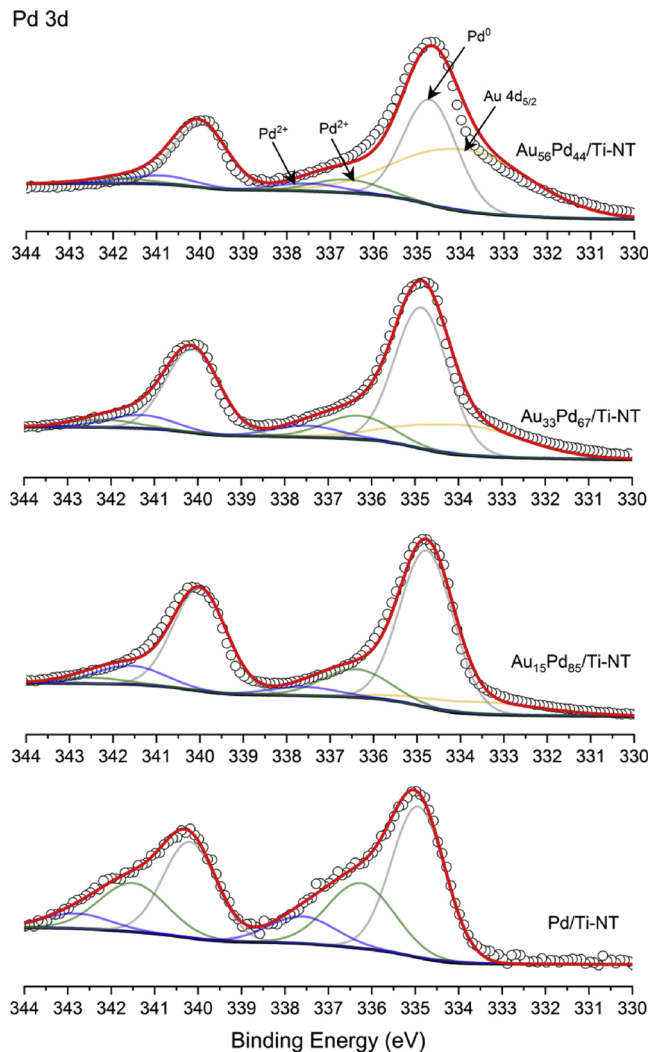


Fig. 4. XPS spectra of Pd 3d for Pd/Ti-NT and $\text{Au}_x\text{Pd}_y/\text{Ti-NT}$ catalysts.

336.3 and 337.6 eV. The portion of metallic and oxidised palladium species present in each catalyst was determined from the fitted Pd 3d spectra and are given in Table 2. The XPS analysis reveals the presence of a high concentration of oxidised palladium species (ca. 43%) on the

surface of catalyst Pd/Ti-NT. The formation of $\text{Pd}^{\delta+}$ species is due to surface oxidation, which mainly arises from drying, transfer and storage of the catalysts. This result is not too surprising since metallic Pd NPs are very prone to oxidation and tend to oxidise readily upon exposure to air. The XPS analysis shows that the introduction of Au to the catalyst leads a significant reduction in the concentration of $\text{Pd}^{\delta+}$ species on the surface, which point to the ligand effect. As the ratio Au/Pd increased, the proportion of Pd^0 species increased with respect to $\text{Pd}^{\delta+}$, so that the catalyst with the highest gold content ($\text{Au}_{56}\text{Pd}_{44}/\text{Ti-NT}$) displayed the lowest concentration of $\text{Pd}^{\delta+}$, as shown in Table 2. This finding is in agreement with a similar observation made by Corma and co-workers [49], in which the presence of Au was found to favour the reduction of $\text{Pd}^{\delta+}$ to Pd^0 even during catalyst drying. Alloyed bimetallic Au-Pd catalysts are also known to exhibit enhanced reducibility and display a lower reduction temperature closer to pure Pd [50].

The atomic surface composition of the catalysts was estimated from the fitted XPS data. The atomic ratio of Au/Pd, and (Au + Pd)/Ti for the different catalysts is given in Table 2. The high Au + Pd/Ti ratio in both the monometallic and bimetallic catalysts implies high metal surface concentration and highlights the advantage of using Ti-NT as a catalyst support. On the other hand, Au-Pd/TiO_2 and Au/TiO_2 displayed significantly lower surface concentrations, Table 2. We have previously shown that a higher metal dispersion and surface concentration can be achieved on Ti-NT in comparison to a conventional TiO_2 nanoparticle support, even while using the same catalyst preparation method (i.e. sol-immobilisation) [51]. The Pd/Au ratio derived from XPS was found to be reasonably close to the bulk ratio determined from ICP, which implies uniform and homogenous Au and Pd dispersion. The slight discrepancy between the two ratios likely reflects the difference in the XPS analysis depth between Au and Pd, and might imply a degree of surface enrichment in the bimetallic Au-Pd NPs. The analysis depth for the Au 4f signal is reportedly 5.4–5.8 nm; and 4.6–5.0 nm for the Pd 3d signal [52]. The difference between the bulk and surface Pd/Au ratios may also reflect the small difference in the surface free energies of Au and Pd [47]. The Pd/Au ratio for catalyst Au-Pd/TiO_2 did not follow the trend observed for $\text{Au}_x\text{Pd}_y/\text{Ti-NT}$. The XPS Pd/Au atomic ratio for this catalyst was found to be considerably larger than the bulk ratio determined by ICP, which in this case probably reflects the poor dispersion and lack of homogenous distribution of Au and Pd on the surface of the support. The low Au surface concentration observed for Au/TiO_2 is a manifestation of the porous structure of the support. It is likely that a large fraction of the Au NPs are within the large pores of the TiO_2 support, and hence become undetectable by XPS surface analysis. In general, the XPS results are in agreement with the metal dispersion results determined from the HRTEM image analysis.

Lastly, no residual Na, B or chloride species were detected by XPS in any of the catalysts, which indicates the full reduction of Au and Pd, and removal of chlorides and Na during catalyst preparation.

3.2. Selective oxidation of glucose

The selective oxidation of glucose was run under initially basic conditions. As noted in the introduction recent developments in recovery of GLA from its Na salt by ion exchange and azeotropic drying [30] may make basic conditions more attractive. Preliminarily studies were performed at various temperatures and oxygen pressures from which it was concluded that $T = 80^\circ\text{C}$, $\text{pH} = 9.5$, and $\text{pO}_2 = 5.0$ barg were ideal for the current study and are similar in terms of temperature and oxygen pressure to the Rennovia patent [24,25]. Therefore, the catalytic performances of the monometallic and bimetallic catalysts were tested under these relatively mild conditions. The two primary products in the selective catalytic oxidation of glucose are gluconic acid (GLO) and glucaric acid (GLA). However, several other side products such as oxalic acid, glycolic acid, 5-ketogluconic acid can also be produced during the oxidation of glucose, as well as the isomerisation

Table 2

XPS Pd 3d and Au 4f binding energies, quantitative XPS data, and atomic ratios for the various catalysts.

Catalyst	(Au + Pd)/Ti ^a	Binding Energy (eV)		Pd 3d ^a		Pd/Au atomic ratio	
		Au ⁰ 4f	Pd ⁰ 3d	Pd ⁰ (%)	Pd ^{δ+} (%) ^b	XPS (surface)	ICP (bulk)
Au/Ti-NT	0.15	83.4	—	—	—	—	—
Pd/Ti-NT	0.34	—	344.9	57.0	43.0	—	—
Au ₅₆ Pd ₄₄ /Ti-NT	0.23	83.3	334.7	80.4	19.6	0.84	0.79
Au ₃₃ Pd ₆₇ /Ti-NT	0.22	83.3	334.9	77.8	22.2	1.66	2.03
Au ₁₅ Pd ₈₅ /Ti-NT	0.28	83.0	334.8	77.7	22.3	4.34	5.67
Au/TiO ₂	0.01	83.3	—	—	—	—	—
Au-Pd/TiO ₂	0.02	83.4	—	—	—	5.17	2.03

^a Values determined from XPS analysis.^b Combined value for Pd²⁺ and Pd⁴⁺ species.

products fructose and mannose. Therefore, maintaining high selectivity and yield of gluconic acid and glucaric acid is important. The oxidation reactions were carried out in batch mode with no adjustment of the pH during the runs. For comparison purposes one run (for Au₅₆Pd₄₄/Ti-NT) was carried out without added base.

3.2.1. Catalytic performance

The glucose conversion and product selectivity are reported in Table 3. In the absence of any catalyst, a glucose conversion of ca. 5.8% was attained due to the isomerisation of glucose to fructose under the mildly basic reaction conditions used in the present study (Table 3). Fructose and mannose are not completely separated by the HPLC column used, especially at these low levels, so that some mannose may be present. The carbon balance was mostly > 92%, as shown in Table 3, which implies that most of the products were detected by HPLC. Part of the missing carbon is due to adsorption of glucose on the Ti-NT support. When the blank Ti-NT support was tested for glucose adsorption, approximately 3.2% of glucose was absorbed by the Ti-NT. The monometallic gold catalyst (i.e Au/Ti-NT) exhibited a conversion of ca. 73% at 6 h and was found to be slightly more active than the bimetallic catalysts. On the other hand, the monometallic palladium catalyst (i.e Pd/Ti-NT) was found to be the least active catalyst among the catalysts prepared by sol-immobilisation. These results show that the addition of a relatively small proportion of Au atoms to Pd NPs can induce a significant enhancement in the catalytic activity. The bimetallic catalysts Au_xPd_y/Ti-NT displayed comparable catalytic activities, but very different extents of oxidation to GLA as discussed below. The catalytic activity of Au/TiO₂ prepared by sol-immobilisation was significantly lower than equivalent catalyst supported on Ti-NT (i.e. Au/Ti-NT). This superior catalytic performance of Ti-NT-supported catalysts in comparison to TiO₂-supported catalysts has been observed previously [45], and was ascribed to the high metal surface concentration (see Table 2), and the ability of the reactants to easily access the highly dispersed

active metal sites on the external surfaces of the support, and the ability of the products to escape. As expected, therefore, the Au/TiO₂ catalyst gave a much lower conversion, while the impregnated catalyst (Au-Pd/TiO₂) displayed even lower activity and was found to be the least active among all the catalysts tested reflecting the relatively poor metal dispersion.

The selectivity to GLO, GLA and the other side products is given in Table 3. At the conditions used all the catalysts gave selectivity to GLO + GLA of > 93%. Catalyst Au₁₅Pd₈₅/Ti-NT exhibited the highest yield and selectivity to GLO, while Au/Ti-NT was found to be the most selective catalyst to GLA. The activity and selectivity of Au catalysts in the oxidation of primary alcoholic groups to the corresponding carboxylates has previously been reported [53] [54]. The bimetallic catalysts Au₅₆Pd₄₄/Ti-NT and Au₃₃Pd₆₇/Ti-NT displayed intermediate selectivity to GLA.

The catalytic activity of the bimetallic catalysts appears to be independent of the Au and Pd atomic composition (Fig. 5a). We have observed similar catalytic activity independent of the Pd/Au ratio in the selective oxidation of salicylic alcohol in presence of a NaOH (see Fig. S5 in the ESI). Notably, the behaviour of bimetallic Au-Pd catalysts observed in the present study for the selective oxidation of glucose and salicylic alcohol in the presence of a base is strikingly different from the well-known volcano-like activity plot observed for the liquid-phase selective oxidation of benzyl alcohol [50,55], which may be related to a promotional role played by the base. On the other hand, the yield to GLA, reflecting the activity for deeper oxidation, is proportional to the atomic concentration of Au in each catalyst, so that a plot of GLA yield against atomic concentration of Au shows a linear correlation (Fig. 5b). This new finding implies that the product selectivity for oxidation to GLA can be controlled by tuning the bimetallic composition of Au_xPd_y/Ti-NT, where deeper oxidation is favoured in Au-rich catalysts (see also Fig. S6 in ESI). An electrocatalytic manganese-based reactor with a similar degree of product versatility was reported recently by Bin et al.

Table 3

Catalytic performance of the various monometallic and bimetallic catalysts in the selective oxidation of glucose.

Catalyst	Conversion ^a (%)	Product selectivity (%) ^a ^b					Carbon balance (%)
		GLO	GLA	GY	OX	FT	
No catalyst	5.8	0	0	0	0	100	0
Pd/Ti-NT	29.6	95.3	2.3	0.6	0	1.8	97.6
Au/Ti-NT	73.0	75.6	18.5	3.0	2.8	0	94.1
Au ₅₆ Pd ₄₄ /Ti-NT	59.7	84.8	13.8	1.2	0.2	0	98.6
Au ₅₆ Pd ₄₄ /Ti-NT (no base)	74.4	93.0	6.1	0.8	0.1	0	100
Au ₃₃ Pd ₆₇ /Ti-NT	57.1	91.3	8.0	0.4	0.2	0	99.3
Au ₁₅ Pd ₈₅ /Ti-NT	64.0	98.1	1.7	0.2	0.1	0	99.8
Au/TiO ₂	9.3	99.9	0	0	0.1	0	99.1
Au-Pd/TiO ₂	5.1	96.7	0.6	2.5	0.2	0	97.3

^a Reaction conditions: T = 80 °C, pO₂ = 5 barg, stirring rate = 1000 rpm, glucose conc. = 0.25 M, pH_{initial} = 9.5, glucose/metal (mol/mol) = 100, Na:glucose (mol/mol) = 1:7900, time = 6 h.

^b Product selectivity: GLO = gluconic acid; GLA = glucaric acid; GY = glycolic acid; OX = oxalic acid; FT = Fructose.

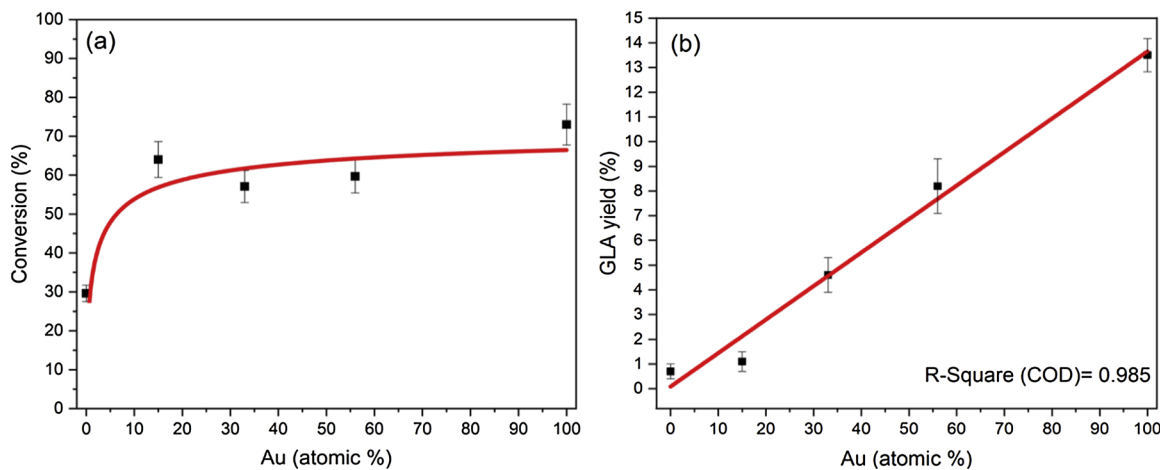


Fig. 5. Conversion as a function of (a) Au atomic content, (b) yield to GLA as function of Au atomic concentration in the catalyst. Reaction conditions: $T = 80^\circ\text{C}$, $\text{pO}_2 = 5$ barg, stirring rate = 1000 rpm, glucose = 0.25 M, $\text{pH}_{\text{initial}} = 9.5$, Na:glucose(mol/mol) = 1:7900, glucose/metal = 100, time = 6 h.

[56], in which the selectivity to GLO and GLA is controlled by varying the density of the electrical current. The correlation of GLA yield with Au content is discussed further in section 3.4 below.

The performance of a Au-Pd catalyst ($\text{Au}_{56}\text{Pd}_{44}/\text{Ti-NT}$) without the addition of NaOH was also investigated. Rather surprisingly, the overall glucose conversion increased. However, the oxidation to GLA was significantly reduced indicating a promoting role of base in the oxidation of GLO to GLA.

3.2.2. Catalytic performance of $\text{Au}_{15}\text{Pd}_{85}/\text{Ti-NT}$ and $\text{Au}/\text{Ti-NT}$

The two most active catalysts, namely $\text{Au}_{15}\text{Pd}_{85}/\text{Ti-NT}$ and $\text{Au}/\text{Ti-NT}$, which present the highest selectivity to GLO ($\text{Au}_{15}\text{Pd}_{85}/\text{Ti-NT}$) and to GLA ($\text{Au}/\text{Ti-NT}$) respectively, were studied further. The catalyst $\text{Au}_{15}\text{Pd}_{85}/\text{Ti-NT}$ and $\text{Au}/\text{Ti-NT}$ were tested over prolonged reaction times to evaluate the evolution of products over time, and to assess their deactivation behaviour. The conversion and selectivity as a function of time for catalysts $\text{Au}_{15}\text{Pd}_{85}/\text{Ti-NT}$ and $\text{Au}/\text{Ti-NT}$ are shown in Fig. 6a and b, respectively. The corresponding product distributions are given in the ESI Tables S1 and S2.

For $\text{Au}/\text{Ti-NT}$, conversion increased continuously with time although a slight deviation from first order kinetics after 6 h, ESI Fig. S7a, is consistent with some deactivation at longer times or inhibition by the adsorption of GLA. The maximum GLO selectivity (ca. 97.2%) was obtained at short reaction times, and subsequently the selectivity decreased to ca. 52% at 20 h as the GLO is further oxidised to GLA. The

oxidation glucose to GLO is faster than the oxidation of GLO to GLA in part due to the lower reactivity of the $-\text{CH}_2\text{OH}$ group present in gluconic acid and the weak ability of GLO to compete with oxygen adsorption [14,26,27,57]. Nonetheless, the monometallic $\text{Au}/\text{Ti-NT}$ catalyst achieved reasonably high yields of GLA under the relatively mild reaction condition used herein ($Y_{\text{GLO}} > 48\%$ and $Y_{\text{GLA}} > 32\%$ at 20 h).

For $\text{Au}_{15}\text{Pd}_{85}/\text{Ti-NT}$, the GLO selectivity was very high (> 99%) up to 2 h reaction time and dropped only slightly (> 96%) at longer times due to the formation of very small amounts of GLA and glycolic acid. Little change in the conversion was observed in the prolonged reaction runs showing the onset of significant catalyst deactivation. This is shown clearly by the good fit to a first-order reaction up 6 h, but deviation thereafter owing to deactivation (Fig. S7b in ESI).

When the initial catalytic activities of $\text{Au}_{15}\text{Pd}_{85}/\text{Ti-NT}$ and $\text{Au}/\text{Ti-NT}$ were compared after one hour of reaction time $\text{Au}/\text{Ti-NT}$ exhibited a higher initial turnover frequency ($\text{TOF} = 29.6 \text{ h}^{-1}$) than $\text{Au}_{15}\text{Pd}_{85}/\text{Ti-NT}$ ($\text{TOF} = 25.8 \text{ h}^{-1}$). These results suggest that $\text{Au}/\text{Ti-NT}$ is intrinsically more active than $\text{Au}_x\text{Pd}_y/\text{Ti-NT}$. Although in the presence of $\text{Au}/\text{Ti-NT}$, the conversion increased to ca. 92% at 20 h, and a higher yield of GLA was obtained, this was accompanied by a significant increase in the formation of oxalic acid and glycolic acid as a result of the consecutive C–C cleavage reactions. Other minor products were also likely produced, but undetected by HPLC resulting in a slightly lower carbon balance (ca. 85.1%).

The catalytic performance of the present $\text{Au}_x\text{Pd}_y/\text{Ti-NT}$ catalysts can

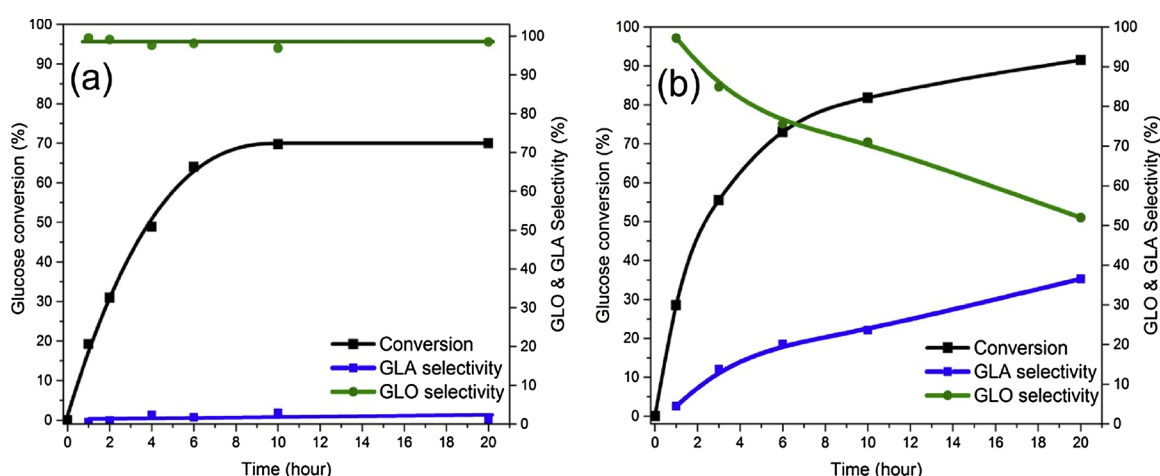


Fig. 6. Glucose conversion and GLO and GLA selectivity for (a) $\text{Au}_{15}\text{Pd}_{85}/\text{Ti-NT}$ and (b) $\text{Au}/\text{Ti-NT}$. Reaction conditions: $T = 80^\circ\text{C}$, $\text{pO}_2 = 5$ barg, stirring rate = 1000 rpm, glucose = 0.25 M, $\text{pH}_{\text{initial}} = 9.5$, glucose/metal = 100, Na:glucose(mol/mol) = 1:7900.

Table 4

Comparison between the catalytic performance of different monometallic and bimetallic catalysts.

Catalyst	pH	T (°C)	P (bar)	Time (h)	Conversion (%)	Selectivity (mol%)		Productivity GLA mol mol ⁻¹ h ⁻¹	Ref.
						GLO	GLA		
Au/Ti-NT ^b	9.5 uncontrolled	80	6.0 O ₂	6	73	75.6	18.5	2.3	This study
Au ₁₅ Pd ₈₅ /Ti-NT ^b	9.5 uncontrolled	80	6.0 O ₂	6	64	98.1	1.7	0.2	This study
Au/TiO ₂ ^b	9.5 uncontrolled	80	6.0 O ₂	6	9.3	99.9	0	0	This study
Pt/C ^c	9.5 uncontrolled	80	6.0 O ₂	10	97	83	16	1.6	This study
Pt/SiO ₂ ^c	9.5 uncontrolled	80	6.0 O ₂	10	45	93	7	0.3	This study
Au/C	9.5 controlled	50	1.0 air	0.5	100	> 99	—	—	[16]
Au-Pt/TiO ₂	7.0 uncontrolled	112	28.6 O ₂	5	100	n/a	n/a	5.8 ^a	[23]
Au-Pt/TiO ₂	7.0 uncontrolled	100	35.5 air	5	n/a	n/a	n/a	2.7 ^a	[58]
Pt/C	8.5 uncontrolled	80	6.2 O ₂	1	100	41	58	31.3 ^a	[27]
Pt ₁ Cu ₃ /TiO ₂	pH > 13 uncontrolled	45	1.0 O ₂	6	100	38	9	15.4 ^a	[26]

^a Values calculated based on data provided in literature.^b Catalyst prepared by sol-immobilisation.^c Catalyst obtained from a commercial vendor.

be compared with various catalysts reported in literature with emphasis on the production of GLA. Since conditions used in the literature vary widely making direct comparison often difficult, 5 wt.% Pt/C and 5 wt.% Pt/SiO₂ commercial catalysts were tested under identical conditions to the Au_xPd_y/Ti-NT catalysts (see Table 4). These catalysts were used directly in their as-received state, except that Pt/SiO₂ was ground to a fine powder before use. It can be seen that Au_xPd_y/Ti-NT offers specific product selectivity which depends on the catalyst composition. This attractive feature makes Au_xPd_y/Ti-NT potentially a very versatile catalyst. It should be noted that the Au/Ti-NT catalyst is selective to GLO (> 97%) either at very short reaction times, Fig. 6b, or at lower reaction temperature (40–50 °C), as expected from results reported for Au/C catalysts [16]. Pt/C and Pt containing catalysts are to date perhaps the most promising in terms of activity and selectivity to GLA and this is clearly shown in Table 4, although interestingly the Au/Ti-NT catalyst is slightly more selective to GLA than the commercial Pt/C catalyst measured under identical conditions. TiO₂-supported bimetallic Pt₁Cu₃ catalysts were recently claimed to be exceptionally active for the oxidation of glucose with a high GLA production rate (see Table 4). However, these catalysts displayed relatively low selectivity to GLO + GLA (< 47%), and produced a large fraction of tartronic and oxalic acids as well as some monocarboxylic acids as a result of the cleavage of C–C bonds [26]. Lee et al. [27] showed that high productivity to GLA can be obtained with Pt/C by careful selection of the reaction conditions.

It is important also to note that the Au-Pd catalysts used in the present work had a considerably lower metal loading (< 2 wt.%) than the Pt catalysts. Higher metal loading can make catalyst deactivation less noticeable. The recycling of Au/Ti-NT and Au₁₅Pd₈₅/Ti-NT is investigated below.

3.3. Catalyst recycling and stability

Catalyst stability and reusability are essential from an application point of view. The catalytic performances of Au₁₅Pd₈₅/Ti-NT and Au/Ti-NT were assessed with repeated usage (Fig. 7). The spent catalysts were recycled after each 6 h run by washing several times with water and ethanol, centrifuging and drying. Catalyst deactivation in liquid-phase oxidation reactions is typically due to one or more of the following reasons: leaching of the active metals, sintering, blocking of the active metal centres by the products (i.e. product inhibition), and/or changes in the oxidation state of the metals.

The recycling study shows a gradual decay in the catalytic activity of Au₁₅Pd₈₅/Ti-NT upon recycling. Despite this noticeable deactivation, Au₁₅Pd₈₅/Ti-NT remained highly selective to GLO upon repeated usage (Fig. 7a). In contrast, the behaviour of Au/Ti-NT with recycling was quite different. Au/Ti-NT was more stable towards deactivation with

recycling as shown Fig. 7b. Interestingly, Au/Ti-NT displayed a slightly higher activity in the 2nd, 3rd and 4th use. This observed enhancement in the activity of Au/Ti-NT is likely due to the partial removal of the capping agent (i.e. PVA) during the first run. We have previously shown that the partial removal of the capping agent in Au_xPd_y/Ti-NT can enhance the catalytic activity [34]. Generally, the presence of the capping agent in the catalyst could be both advantageous and undesirable. While it provides stability to the catalyst by preventing the coalescence of the metal NPs, it can also become detrimental to the catalytic activity by shielding the active catalytic centres [59]. Another plausible reason for the slight enhancement in the catalytic activity of Au/Ti-NT upon recycling is related to the growth of the Au particle size. While the Au/Ti-NT catalyst prepared in the current study exhibits an average Au particle size of ca. 3.2 nm, recent studies suggest that the optimal Au particle size for glucose oxidation might be around 7.0 nm [60,61]. Li et al. [62] also recently studied the catalytic activity of well-defined gold nanoclusters on carbon (Au_n/C, n = 25–144 atoms) in the oxidation of glucose, and found the activity to be size-dependent with the larger nanoclusters displaying higher activity. Hence, the observed enhancement in the catalytic activity after the first catalytic cycle may also be ascribed in part to the enlargement in the Au particle size.

Several studies have reported that metal leaching is the primary reason for catalytic deactivation of noble metal-based catalysts in the oxidation of glucose [11,17,60]. At uncontrolled pH reaction conditions such as used here, the pH of the reaction mixture falls gradually as conversion increases, reaching a pH of about 5 after 10 h of reaction time. In addition, glucose and the product acids are strong chelating agents and can mediate the leaching of active metal components during the reaction. In the present study, the spent Au₁₅Pd₈₅/Ti-NT and Au/Ti-NT catalysts were analysed by ICP in order to determine the total metal loss after cycling (see Table 5). For the bimetallic catalyst (Au₁₅Pd₈₅/Ti-NT), the amount of Pd lost was ca. 58% of the initial Pd loading, while Au lost 47% of its initial loading after four cycles. In comparison, the Au lost from catalyst Au/Ti-NT was about 37% of the initial loading after the five cycles. As expected, the rate of leaching is higher for Pd than Au.

Analysis of the spent catalysts by XPS (Figs. 8 and 9) did not show any major changes in the oxidation state of Au or Pd with cycling, which excludes alteration in the metallic state as a reason for the observed catalytic deactivation. Remarkably, the Pd 3d XPS spectra for the recycled Au₁₅Pd₈₅/Ti-NT catalyst did not show evidence of Pd over-oxidation likely as a consequence of alloying with Au, which protects Pd from oxidation.

The atomic surface composition of Au and Pd in the spent catalysts did not correlate with the bulk composition, and was found to be significantly lower than the XPS surface composition of the fresh catalysts (Tables 2 and 4), which implies lower metal dispersion, as a result of

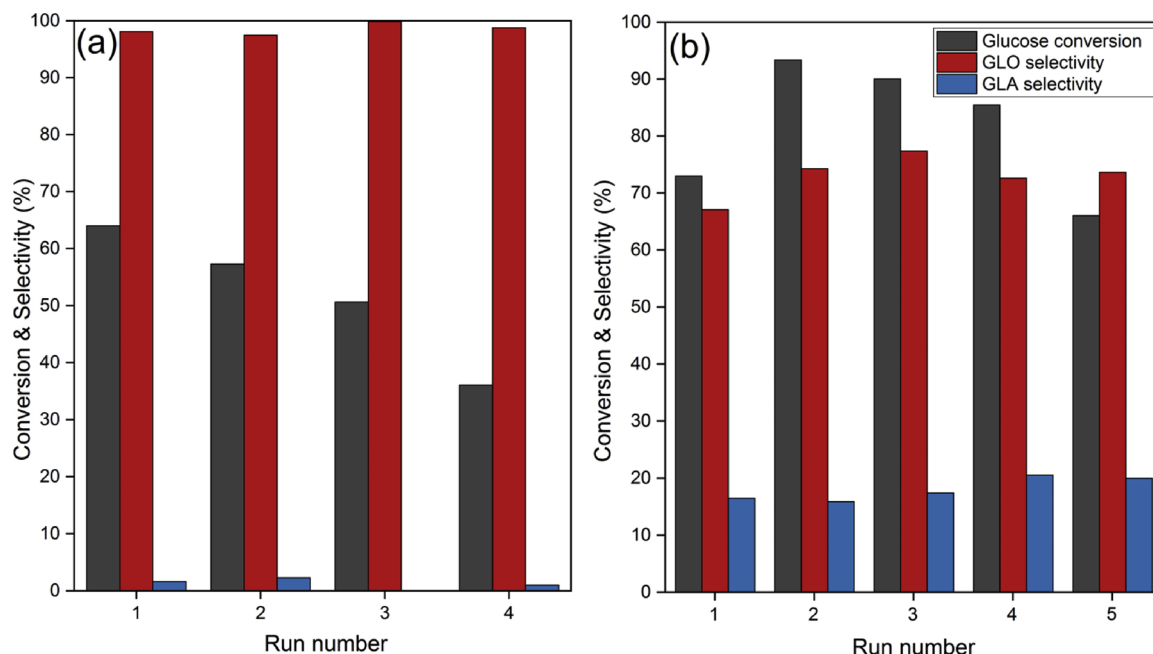


Fig. 7. Recycling studies of (a) $\text{Au}_{15}\text{Pd}_{85}/\text{Ti-NT}$ and (b) $\text{Au}/\text{Ti-NT}$. Reaction conditions: $T = 80^\circ\text{C}$, $p\text{O}_2 = 5$ barg, stirring rate = 1000 rpm, glucose = 0.25 M, $\text{pH}_{\text{initial}} = 9.5$, glucose/metal = 100, Na:glucose(mol/mol) = 1:7900, time = 6 h.

Table 5
Bulk and XPS surface metal composition for spent catalysts.

Catalyst	Au ^a (wt.%)		Pd ^a (wt.%)		(Au + Pd)/Ti ^b	
	Fresh	Spent	Fresh	Spent	Fresh	Spent
$\text{Au}_{15}\text{Pd}_{85}/\text{Ti-NT}$	0.46	0.24 ^c	1.37	0.53 ^c	0.28	0.02 ^c
$\text{Au}/\text{Ti-NT}$	1.61	1.01 ^d	–	–	0.15	0.03 ^d

^a Bulk composition; weight percentage per gram of sample, obtained by ICP-AES analysis.

^b Determined by XPS.

^c Spent catalyst analysed after 4 catalytic cycles.

^d Spent catalyst analysed after 5 catalytic cycles.

the aggregation of the metal NPs as confirmed by TEM analysis of the spent catalyst (See Fig. S8 in ESI).

The C1 s XPS spectra for the spent catalysts are shown in Figs. 8c and 9b for catalysts $\text{Au}_{15}\text{Pd}_{85}/\text{Ti-NT}$ and $\text{Au}/\text{Ti-NT}$, respectively. The C1 s spectra can be deconvoluted into three peaks; the first peak is located at 284.8 eV and corresponds to C–H and C–C bonds, the second peak is found at ca. 286.2 eV and is assigned to the C–O bonds, and the last peak is located at ca. 289.0 and is assigned to C=O bonds [60]. The increase in the relative intensity of the peaks assigned to the C–O and C=O bonds is most noticeable for catalyst $\text{Au}/\text{Ti-NT}$ (Fig. 9d), and can be ascribed to the adsorption of the highly oxygenated reaction products such as glucaric and oxalic acids. The C/Ti ratio for the fresh and spent catalysts is given in Tables S5 and S6, and indicates the presence of higher amounts of organic carbon on the surface of the catalyst. The higher O/C ratio for the spent catalysts also suggests enrichment in oxygen-containing products, see Table S5 and S6. These results are in agreement with our previous infrared spectroscopy (IR) study of spent $\text{Au}_x\text{Pd}_y/\text{Ti-NT}$ catalysts [34], in which the strong adsorption of oxygenated products was shown to be partially responsible for catalyst deactivation. The reduction in XPS intensity from C–C bonds in the spent catalyst sample $\text{Au}_{15}\text{Pd}_{85}/\text{Ti-NT}$ is due to the further removal of the PVA ligand and is also consistent with the high metal leaching observed for this catalyst.

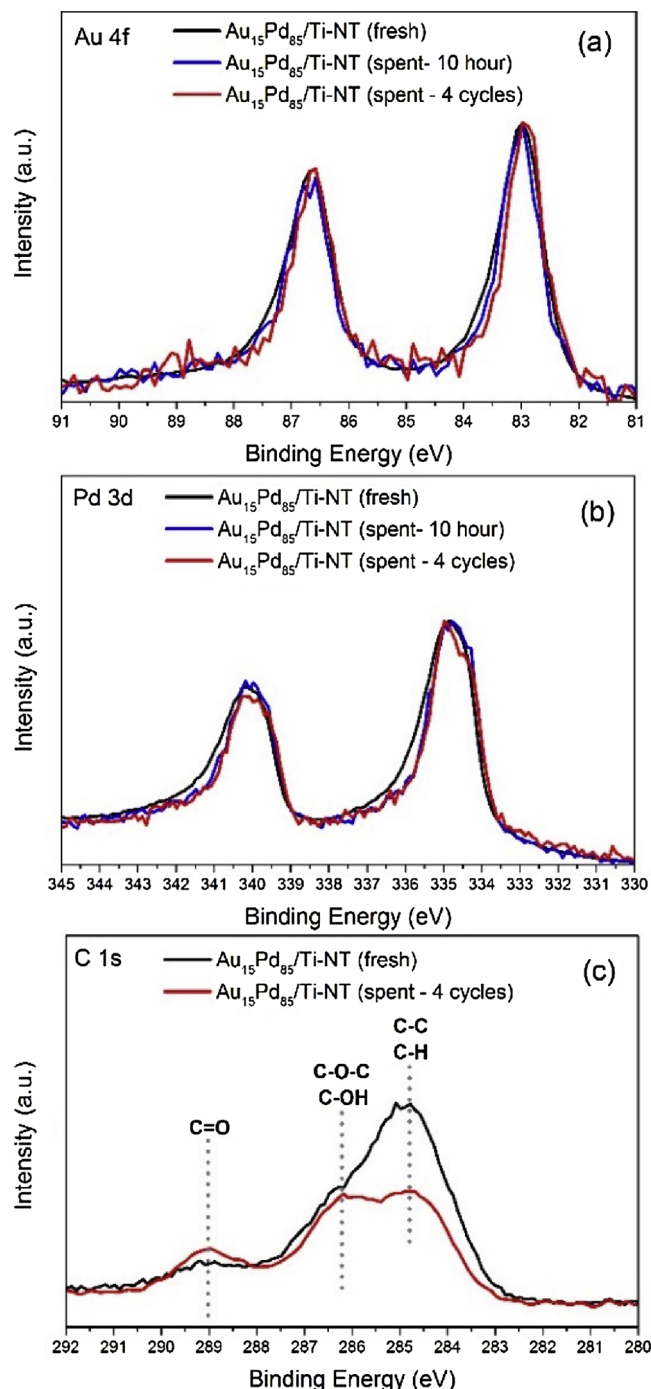
It is known that there is a considerably reduced level of leaching of Au at pH = 9 and above. To confirm that the present Au catalyst would

be stable in controlled pH conditions, we tested the $\text{Au}/\text{Ti-NT}$ catalyst at pH = 9.5, $T = 80^\circ\text{C}$ with continuous flow of oxygen at atmospheric pressure and addition of NaOH controlled by a Mettler-Toledo Titrando auto-titrator system. Under these conditions of low oxygen pressure and high pH there was significant glucose isomerisation to fructose initially in addition to selective oxidation (Fig. S9). Crucially, however, analysis of the spent catalyst revealed negligible metal leaching (less than 10% of the original Au loading).

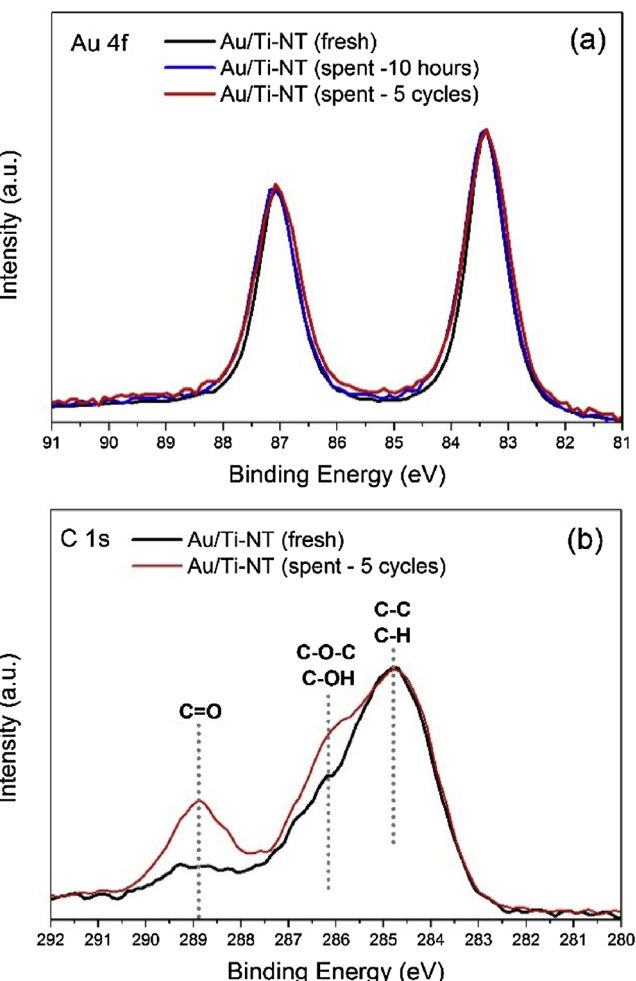
3.4. Catalytic activity of leached material

The observation of significant leaching raises the possibility of a contribution of leached species to the observed catalytic activity, especially in the light of recent work on the activity of solubilized Au clusters [63]. The possible activity of leached species was investigated in the following way. The experiment was conducted using an Au-Pd catalyst ($\text{Au}_{56}\text{Pd}_{44}/\text{Ti-NT}$, see Table 1) in the presence of glucose at the standard reaction conditions (0.25 M with pH 9.5, at 80°C , 6 bar O_2 , 6 h), see entry 1 in Table 6. After the reaction, the catalyst was removed from the liquid by centrifugation, and the liquid filtered with a syringe filter (0.2 μm). Analysis of the spent catalyst showed considerable metal loss due to leaching during the reaction (Au = 0.88 wt.%, Pd = 0.36 wt.%). Subsequently, the recovered product liquid was added back to the reactor, the pH was adjusted to 9.5, and the reaction liquid was reacted at $p\text{O}_2 = 5$ barg and 80°C for a further 6 h. Analysis of the reaction products did not show any increase in the glucose conversion. However, there was a significant increase in the conversion of GLO to GLA (entry 2 in Table 6).

When Au or Au-Pd catalysts were exposed to just DI water (no glucose) at the standard conditions, and subsequently the catalyst was removed and glucose was added to the recovered liquid, a glucose conversion of only ca. 1% was obtained, where GLO was the only identified product. Analysis of the spent catalysts from the water leaching experiments showed no evidence of metal loss. These results clearly indicate that glucose and the reaction products, in particular GLO and GLA, were acting as chelating agents and are evidently involved in the observed metal leaching. Furthermore, the leached material is clearly catalytically active for the conversion of GLO to GLA i.e. the deeper oxidation step.



The above results and the correlation of GLA yield with Au content, Fig. 5b, can also be understood in terms of a significant contribution to the observed activity by leached Au species. Unsupported Au and Au-Pd colloidal NPs have previously been reported to catalyse the aerobic oxidation of glucose [64]. More importantly, recent studies have shown that solubilized atomic Au clusters $< 1.0 \text{ nm}$ in size present in concentrations as low as ng/mL have the ability to activate molecular oxygen and initiate oxidation reactions [63]. Oxygenated compounds were shown to act as chelating agents and facilitate the dissolution of Au clusters from larger Au NPs. For these reasons, it seems probable that a similar phenomenon exists in the present Au-Pd catalytic system. The efficiency of production of Au clusters can be expected to be related



to a range of catalyst properties. Hence the apparent correlations between catalyst properties such as metal dispersion, alloying, surface concentration etc. and catalytic activity. Furthermore, since one might expect solubilized clusters to ripen as time passes, the presence of the heterogeneous catalyst is probably essential for sustained activity to provide a continuous supply of new clusters. The results here are preliminary and further work is necessary to fully elucidate the role of Au clusters in the oxidation of glucose.

4. Conclusion

In this work, we have demonstrated the catalytic activity and selectivity of $\text{Au}/\text{Ti-NT}$ and $\text{Au}_x\text{Pd}_y/\text{Ti-NT}$ catalysts for the selective oxidation of glucose using O_2 under relatively mild conditions. The catalytic performance of the various AuPd catalysts was found to be strongly dependent on the bimetallic composition. Au-rich catalysts were found to favour deep oxidation to glucaric acid while Pd-rich catalysts favoured the formation of gluconic acid. The catalytic activity of the Au-Pd catalysts did not show strong dependency on the bimetallic composition, while the monometallic Pd/Ti-NT catalyst displayed very low catalytic activity. The addition of as low as 15 atomic % of Au to the Pd NPs led to a substantial enhancement in the catalytic activity due to the formation of AuPd alloys leading to a linear correlation between the yield of glucaric acid and Au content. These findings suggest that the bimetallic composition of $\text{Au}_x\text{Pd}_y/\text{Ti-NT}$ can be tuned to enhance the production of either gluconic acid or glucaric acid.

While the catalytic performance of $\text{Au}/\text{Ti-NT}$ and $\text{Au}_x\text{Pd}_y/\text{Ti-NT}$ is promising, catalyst deactivation mainly due to metal leaching was

Table 6Homogeneous contribution to glucose oxidation for Au₅₆Pd₄₄/Ti-NT.

Entry	Conversion ^a (%)	Product selectivity (%) ^{a, b}						Carbon balance (%)
		GLO	GLA	GY	OX	FT	GLO + GLA	
1 Run with Au ₅₆ Pd ₄₄ /Ti-NT	58.2	87.4	11.9	0.6	0.1	0	99.3	101
2 Run of recovered liquid	57.6	62.8	36.0	1.2	0	0	98.8	97

^a Reaction conditions: T = 80 °C, pO₂ = 5 barg, pH = 9.5, stirring rate = 1000 rpm.^b Product selectivity: GLO = gluconic acid; GLA = glucaric acid; GY = glycolic acid; OX = oxalic acid; FT = Fructose.

significant as a consequence of the uncontrolled pH of the reaction mixture which becomes acidic as the reaction proceeds to high conversion. Under application of controlled pH leaching would be minimised, and this was confirmed in a preliminary study. Leached species were found to be active for the oxidation of gluconic acid to glucaric acid, which together with the linear correlation of glucaric acid yield with catalyst Au content, suggests that gold clusters play a significant role in the oxidation as recently reported for selective oxidation reactions [63].

Acknowledgment

Motaz Khawaji gratefully acknowledges the financial support of Saudi Aramco. This work was funded by EPSRCEP/K014749/1. We thank Katty Elizabeth Cabezas Terán for assistance with preliminary measurements on glucose oxidation, and Babajide Aina and Li Lyu for help in carrying out some of the catalytic activity measurements on salicyl alcohol. We are grateful to Professor Graham Hutchings and Dr. Robert Armstrong from Cardiff Catalysis Institute for providing us with a sample of glucaric acid.

Appendix A. Supplementary data

Supplementary material related to this article can be found, in the online version, at doi:<https://doi.org/10.1016/j.apcatb.2019.117799>.

References

- J.N. Chheda, G.W. Huber, J.A. Dumesic, Liquid-phase catalytic processing of biomass-derived oxygenated hydrocarbons to fuels and chemicals, *Angew. Chemie Int. Ed.* 46 (2007) 7164–7183.
- A.M. Cafete-Rodríguez, I.M. Santos-Dueñas, J.E. Jiménez-Hornero, A. Ehrenreich, W. Liebl, I. García-García, Gluconic acid: properties, production methods and applications—an excellent opportunity for agro-industrial by-products and waste valorization, *Process. Biochem.* 51 (2016) 1891–1903.
- Y. Önal, S. Schimpf, P. Claus, Structure sensitivity and kinetics of d-glucose oxidation to d-gluconic acid over carbon-supported gold catalysts, *J. Catal.* 223 (2004) 122–133.
- N. Thielecke, M. Aytemir, U. Prüsse, Selective oxidation of carbohydrates with gold catalysts: continuous-flow reactor system for glucose oxidation, *Catal. Today* 121 (2007) 115–120.
- M. Comotti, C.D. Pina, M. Rossi, Mono- and bimetallic catalysts for glucose oxidation, *J. Mol. Catal. A Chem.* 251 (2006) 89–92.
- T. Werpy, G. Petersen, A. Aden, J. Bozell, J. Holladay, J. White, A. Manheim, D. Eliot, L. Lasure, S. Jones, Top value added chemicals from biomass, Volume 1 - Results of Screening for Potential Candidates From Sugars and Synthesis Gas, (2004).
- F.H. Isikgor, C.R. Becer, Lignocellulosic biomass: a sustainable platform for the production of bio-based chemicals and polymers, *Polym. Chem.* 6 (2015) 4497–4559.
- D.E. Kiely, L. Chen, T.H. Lin, Hydroxylated nylons based on unprotected esterified D-glucaric acid by simple condensation reactions, *J. Am. Chem. Soc.* 116 (1994) 571–578.
- C.L. Mehlretter, Process of Making D-saccharic Acid, US Patents (1948).
- C.L. Mehlretter, C.E. Rist, Sugar Oxidation, Saccharic and oxalic acids by the nitric acid oxidation of dextrose, *J. Agric. Food Chem.* 1 (1953) 779–783.
- E. Derrien, M. Mounguengui-Diallo, N. Perret, P. Marion, C. Pinel, M. Besson, Aerobic oxidation of glucose to glucaric acid under alkaline-free conditions: Au-Based bimetallic catalysts and the effect of residues in a hemicellulose hydrolysate, *Ind. Eng. Chem. Res.* 56 (2017) 13175–13189.
- K. Deller, H. Krause, E. Peldszus, B. Despeyroux, Method for Preparation of Gluconic Acid by Catalytic Oxidation of Glucose, US Patents (1992).
- M. Besson, F. Lahmer, P. Gallezot, P. Fuertes, G. Fleche, Catalytic oxidation of glucose on bismuth-promoted palladium catalysts, *J. Catal.* 152 (1995) 116–121.
- J.M.H. Dirkx, H.S. van der Baan, The oxidation of gluconic acid with platinum on carbon as catalyst, *J. Catal.* 67 (1981) 14–20.
- H. Zhang, N. Toshima, Glucose oxidation using Au-containing bimetallic and trimetallic nanoparticles, *Catal. Sci. Technol.* 3 (2013) 268–278.
- S. Biella, L. Prati, M. Rossi, Selective oxidation of D-Glucose on gold catalyst, *J. Catal.* 206 (2002) 242–247.
- A. Mirescu, U. Prüsse, A new environmental friendly method for the preparation of sugar acids via catalytic oxidation on gold catalysts, *Appl. Catal. B* 70 (2007) 644–652.
- C. Megias-Sayago, S. Ivanova, C. López-Cartes, M.A. Centeno, J.A. Odriozola, Gold catalysts screening in base-free aerobic oxidation of glucose to gluconic acid, *Catal. Today* 279 (2017) 148–154.
- R. Wojcieszak, I.M. Cuccova, M.A. Silva, L.M. Rossi, Selective oxidation of glucose to glucuronic acid by cesium-promoted gold nanoparticle catalyst, *J. Mol. Catal. A Chem.* 422 (2016) 35–42.
- S. Hermans, M. Devillers, On the role of ruthenium associated with Pd and/or Bi in carbon-supported catalysts for the partial oxidation of glucose, *Appl. Catal. A Gen.* 235 (2002) 253–264.
- Y. Cao, X. Liu, S. Iqbal, P.J. Miedziak, J.K. Edwards, R.D. Armstrong, D.J. Morgan, J. Wang, G.J. Hutchings, Base-free oxidation of glucose to gluconic acid using supported gold catalysts, *Catal. Sci. Technol.* 6 (2016) 107–117.
- M. Besson, P. Gallezot, C. Pinel, Conversion of biomass into chemicals over metal catalysts, *Chem. Rev.* 114 (2014) 1827–1870.
- V.J. Murphy, J. Shoemaker, G. Zhu, R. Archer, G.F. Salem, E.L. Dias, Oxidation Catalysts, US Patents (2011).
- T.R. Boussie, E.L. Dias, Z.M. Fresco, V.J. Murphy, Production of Adipic Acid and Derivatives From Carbohydrate-containing Materials, US Patents (2013).
- T.R. Boussie, E.L. Dias, Z.M. Fresco, V.J. Murphy, Production of Adipic Acid and Derivatives From Carbohydrate-containing Materials, US Patents (2015).
- X. Jin, M. Zhao, J. Shen, W. Yan, L. He, P.S. Thapa, S. Ren, B. Subramanian, R.V. Chaudhari, Exceptional performance of bimetallic Pt1Cu3/TiO2 nanocatalysts for oxidation of gluconic acid and glucose with O₂ to glucaric acid, *J. Catal.* 330 (2015) 323–329.
- J. Lee, B. Saha, D.G. Vlachos, Pt catalysts for efficient aerobic oxidation of glucose to glucaric acid in water, *Green Chem.* 18 (2016) 3815–3822.
- D. Armstrong Robert, M. Kariuki Benson, W. Knight David, J. Hutchings Graham, How to synthesise high purity, crystalline d-Glucaric acid selectively, *European J. Org. Chem.* 2017 (2017) 6811–6814.
- Z. Zhang, P. Gibson, S.B. Clark, G. Tian, P.L. Zanonato, L. Rao, Lactonization and protonation of gluconic acid: a thermodynamic and kinetic study by Potentiometry, NMR and ESI-MS, *J. Solution Chem.* 36 (2007) 1187–1200.
- R.D. Armstrong, S.J. Freakley, M.J. Forde, V. Peneau, R.L. Jenkins, S.H. Taylor, J.A. Moulijn, D.J. Morgan, G.J. Hutchings, Low temperature catalytic partial oxidation of ethane to oxygenates by Fe- and Cu-ZSM-5 in a continuous flow reactor, *J. Catal.* 330 (2015) 84–92.
- M. Comotti, C. Della Pina, R. Matarrese, M. Rossi, The catalytic activity of “Naked” gold particles, *Angew. Chemie* 116 (2004) 5936–5939.
- C. Baatz, N. Thielecke, U. Prüsse, Influence of the preparation conditions on the properties of gold catalysts for the oxidation of glucose, *Appl. Catal. B* 70 (2007) 653–660.
- T. Ishida, N. Kinoshita, H. Okatsu, T. Akita, T. Takei, M. Haruta, Influence of the support and the size of gold clusters on catalytic activity for glucose oxidation, *Angew. Chemie Int. Ed.* 47 (2008) 9265–9268.
- M. Khawaji, D. Chadwick, Au-Pd bimetallic nanoparticles immobilised on titanate nanotubes: a highly active catalyst for selective oxidation, *ChemCatChem* 9 (2017) 4353–4363.
- D.V. Bavykin, F.C. Walsh, Titanate and Titania Nanotubes : Synthesis, Properties and Applications, (2009).
- M. Khawaji, D. Chadwick, Selective catalytic oxidation over Au-Pd/titanate nanotubes and the influence of the catalyst preparation method on the activity, *Catal. Today* (2018).
- T. Kasuga, M. Hiramatsu, A. Hoson, T. Sekino, K. Niihara, Formation of titanium oxide nanotube, *Langmuir* 14 (1998) 3160–3163.
- N. Dimitratos, J.A. Lopez-Sanchez, D. Morgan, A.F. Carley, R. Tiruvalam, C.J. Kiely, D. Bethell, G.J. Hutchings, Solvent-free oxidation of benzyl alcohol using Au-Pd catalysts prepared by sol immobilisation, *Phys. Chem. Chem. Phys.* 11 (2009) 5142–5153.
- J. Regalbuto, Catalyst Preparation Science and Engineering, CRC Press, Boca Raton, 2007.
- E. Morgado, M.A.S. de Abreu, O.R.C. Pravia, B.A. Marinkovic, P.M. Jardim,

F.C. Rizzo, A.S. Araújo, A study on the structure and thermal stability of titanate nanotubes as a function of sodium content, *Solid State Sci.* 8 (2006) 888–900.

[41] R.A. Ortega-Domínguez, J.A. Mendoza-Nieto, P. Hernández-Hipólito, F. Garrido-Sánchez, J. Escobar-Aguilar, S.A.I. Barri, D. Chadwick, T.E. Klimova, Influence of Na content on behavior of NiMo catalysts supported on titania nanotubes in hydrodesulfurization, *J. Catal.* 329 (2015) 457–470.

[42] B. Pawelec, A.M. Venezia, V. La Parola, E. Cano-Serrano, J.M. Campos-Martin, J.L.G. Fierro, AuPd alloy formation in Au-Pd/Al2O3 catalysts and its role on aromatics hydrogenation, *Appl. Surf. Sci.* 242 (2005) 380–391.

[43] E.G. Allison, G.C. Bond, The structure and catalytic properties of palladium-silver and palladium-gold alloys, *Catal. Rev.* 7 (1972) 233–289.

[44] Y.-F. Han, Z. Zhong, K. Ramesh, F. Chen, L. Chen, T. White, Q. Tay, S.N. Yaakub, Z. Wang, Au promotional effects on the synthesis of H2O2 directly from H2 and O2 on supported Pd–Au alloy catalysts, *J. Phys. Chem. C* 111 (2007) 8410–8413.

[45] M. Khawaji, D. Chadwick, Au-Pd NPs immobilised on nanostructured ceria and titania: impact of support morphology on the catalytic activity for selective oxidation, *Catal. Sci. Technol.* 8 (2018) 2529–2539.

[46] K. Mori, T. Hara, T. Mizugaki, K. Ebitani, K. Kaneda, Hydroxyapatite-supported palladium nanoclusters: a highly active heterogeneous catalyst for selective oxidation of alcohols by use of molecular oxygen, *J. Am. Chem. Soc.* 126 (2004) 10657–10666.

[47] C.W. Yi, K. Luo, T. Wei, D.W. Goodman, The composition and structure of Pd–Au surfaces, *J. Phys. Chem. B* 109 (2005) 18535–18540.

[48] A. Villa, N. Dimitratos, C.E. Chan-Thaw, C. Hammond, G.M. Veith, D. Wang, M. Manzoli, L. Prati, G.J. Hutchings, Characterisation of gold catalysts, *Chem. Soc. Rev.* 45 (2016) 4953–4994.

[49] P. Concepción, S. García, J.C. Hernández-Garrido, J.J. Calvino, A. Corma, A promoting effect of dilution of Pd sites due to gold surface segregation under reaction conditions on supported Pd–Au catalysts for the selective hydrogenation of 1,5-cyclooctadiene, *Catal. Today* 259 (2016) 213–221.

[50] J.H. Carter, S. Althahban, E. Nowicka, S.J. Freakley, D.J. Morgan, P.M. Shah, S. Golunski, C.J. Kiely, G.J. Hutchings, Synergy and anti-synergy between palladium and gold in nanoparticles dispersed on a reducible support, *ACS Catal.* 6 (2016) 6623–6633.

[51] M. Khawaji, D. Chadwick, Au-Pd NPs immobilised on nanostructured ceria and titania: impact of support morphology on the catalytic activity for selective oxidation, *Catal. Sci. Technol.* 8 (2018) 2529–2539.

[52] C.M. Olmos, L.E. Chinchilla, A. Villa, J.J. Delgado, H. Pan, A.B. Hungría, G. Blanco, J.J. Calvino, L. Prati, X. Chen, Influence of pretreatment atmospheres on the performance of bimetallic Au-Pd supported on ceria-zirconia mixed oxide catalysts for benzyl alcohol oxidation, *Appl. Catal. A Gen.* 525 (2016) 145–157.

[53] C. Bianchi, F. Porta, L. Prati, M. Rossi, Selective liquid phase oxidation using gold catalysts, *Top. Catal.* 13 (2000) 231–236.

[54] L. Prati, M. Rossi, Chemoselective catalytic oxidation of polyols with dioxygen on gold supported catalysts, in: R.K. Grasselli, S.T. Oyama, A.M. Gaffney, J.E. Lyons (Eds.), *Studies in Surface Science and Catalysis*, Elsevier, 1997, pp. 509–516.

[55] T.A.G. Silva, E. Teixeira-Neto, N. López, L.M. Rossi, Volcano-like behavior of Au-Pd core-shell nanoparticles in the selective oxidation of alcohols, *Sci. Rep.* 4 (2014) 5766.

[56] D. Bin, H. Wang, J. Li, H. Wang, Z. Yin, J. Kang, B. He, Z. Li, Controllable oxidation of glucose to gluconic acid and glucaric acid using an electrocatalytic reactor, *Electrochim. Acta* 130 (2014) 170–178.

[57] J.M.H. Dirkx, H.S. van der Baan, The oxidation of glucose with platinum on carbon as catalyst, *J. Catal.* 67 (1981) 1–13.

[58] T.R. Boussie, E.L. Dias, Z.M. Fresco, V.J. Murphy, J. Shoemaker, R. Archer, H. Jiang, Production of Adipic Acid and Derivatives from Carbohydrate-Containing Materials, RENNOVIA Inc, 2014 USP US8,669,397 B2.

[59] A. Villa, D. Wang, G.M. Veith, F. Vindigni, L. Prati, Sol immobilization technique: a delicate balance between activity, selectivity and stability of gold catalysts, *Catal. Sci. Technol.* 3 (2013) 3036.

[60] C. Megías-Sayago, L.F. Bobadilla, S. Ivanova, A. Penkova, M.A. Centeno, J.A. Odriozola, Gold catalyst recycling study in base-free glucose oxidation reaction, *Catal. Today* 301 (2018) 72–77.

[61] L. Prati, A. Villa, A.R. Lupini, G.M. Veith, Gold on carbon: one billion catalysts under a single label, *J. Chem. Soc. Faraday Trans.* 14 (2012) 2969–2978.

[62] J. Zhang, Z. Li, J. Huang, C. Liu, F. Hong, K. Zheng, G. Li, Size dependence of gold clusters with precise numbers of atoms in aerobic oxidation of d-glucose, *Nanoscale* 9 (2017) 16879–16886.

[63] L. Qian, Z. Wang, E.V. Beletskiy, J. Liu, H.J. dos Santos, T. Li, Md.C. Rangel, M.C. Kung, H.H. Kung, Stable and solubilized active Au atom clusters for selective epoxidation of cis-cyclooctene with molecular oxygen, *Nat. Commun.* 8 (2017) 14881.

[64] H. Zhang, L. Wang, L. Lu, N. Toshima, Preparation and catalytic activity for aerobic glucose oxidation of crown jewel structured Pt/Au bimetallic nanoclusters, *Sci. Rep.* 6 (2016) 30752.